



| | |
|----------------------------------|--|
| Publication Year | 2020 |
| Acceptance in OA | 2025-03-14T17:01:39Z |
| Title | X-ray processing of a realistic ice mantle can explain the gas abundances in protoplanetary disks |
| Authors | CIARAVELLA, Angela, Muñoz Caro, Guillermo M., JIMENEZ ESCOBAR, Antonio, CECCHI PESTELLINI, Cesare, Hsiao, Li-Chieh, Huang, Chao-Hui, Chen, Yu-Jung |
| Publisher's version (DOI) | 10.1073/pnas.2005225117 |
| Handle | http://hdl.handle.net/20.500.12386/36822 |
| Journal | PROCEEDINGS OF THE NATIONAL ACADEMY OF SCIENCES OF THE UNITED STATES OF AMERICA |
| Volume | 117 |

X-ray processing of a realistic ice mantle can explain the gas abundances in protoplanetary disks

Angela Ciaravella^{a,1}, Guillermo M. Muñoz Caro^b, Antonio Jiménez-Escobar^a, Cesare Cecchi-Pestellini^a, Li-Chieh Hsiao^c, Chao-Hui Huang^c, and Yu-Jung Chen^c

^aINAF - Osservatorio Astronomico di Palermo, P.zza Parlamento 1, 90134 Palermo, Italy; ^bCentro de Astrobiología (INTA-CSIC), Carretera de Ajalvir, km 4, Torrejón de Ardoz, 28850 Madrid, Spain; ^cDepartment of Physics, National Central University, Zhongli City, Taoyuan County 32054, Taiwan

This manuscript was compiled on May 20, 2020

1 **The Atacama Large Millimeter Array has allowed a detailed observa-**
2 **tion of molecules in protoplanetary disks, which can evolve toward**
3 **solar systems like our own. While CO, CO₂, HCO, and H₂CO are often**
4 **abundant species in the cold zones of the disk, CH₃OH or CH₃CN are**
5 **only found in a few regions, and more complex organic molecules are**
6 **not observed. We simulate experimentally ice processing in disks**
7 **under realistic conditions, i.e. layered ices irradiated by soft X-rays.**
8 **X-ray emission from young solar-type stars is thousands of times**
9 **brighter than that of today Sun. The ice mantle is composed of a**
10 **H₂O:CH₄:NH₃ mixture, covered by a layer made of CH₃OH and CO.**
11 **The photo-products found desorbing from both ice layers to the gas-**
12 **phase during the irradiation converge with those detected in higher**
13 **abundances in the gas phase of protoplanetary disks, providing im-**
14 **portant insights on the non-thermal processes that drive the chem-**
15 **istry in these objects.**

astrochemistry | protoplanetary disks | X-rays | methods: laboratory:
molecular

1 **I**ce mantles covering (sub-)micron dust grains in interstellar
2 and protoplanetary environments are mainly composed of
3 simple species in a water-dominated ice. Hydrogenation of
4 O, C, and N on the grain surface produces a first layer of
5 water (H₂O), methane (CH₄), ammonia (NH₃), and other
6 reduced species. On top of this, there is a second layer of
7 species that are formed in the gas phase and require lower
8 temperatures to stick onto the dust, being carbon monoxide
9 (CO) the most abundant component (1–3). The coalescence of
10 CO with methanol (CH₃OH) in these ices is inferred from the
11 fit of the CO ice band profile near 4.6 micron observed in the
12 infrared (4). The hydrogenation of CO molecules in these ices
13 is proposed as a plausible formation mechanism for CH₃OH (5).
14 Most experimental simulations of astrophysical ice processing
15 with an energy source were conducted with either pure or
16 binary ice analogs to understand the photolysis and radiolysis
17 of molecules and the product formation (6). Multicomponent
18 ice mixtures were also explored to mimic the formation of
19 complex organic molecules (COMs) in the ice, in particular
20 those remaining in the residue at room temperature after
21 warm-up of ultraviolet or ion-processed ices. Since amino acids,
22 sugars, nucleobases, and other prebiotic species are among the
23 products of ice irradiation, these studies are of interest to a
24 broad scientific community (7–11). More recently, COMs were
25 also produced as the result of X-ray irradiation of ice analog
26 mixtures (12, 13).

27 **Here we report the first experimental simulation**
28 **of a more astrophysically realistic ice mantle mor-**
29 **phology, organized in a bi-layered structure of seg-**
30 **regated polar and apolar components (14, 15). The**
31 **selected relative abundances of the ice species are sim-**

ilar to previous experimental works dedicated to ul-
traviolet irradiation of ice mixtures (10, 16, 17) but
none of these works segregated the molecular species
into distinct polar and apolar ice layers. This ice
composition was inferred from astronomical observa-
tions (3), and it is closer to the abundances found
around protostellar sources (18, 19). Indeed, the line
of sight abundances of CH₃OH and CO₂ are about
5 – 10 times lower than the abundances found close
to the protostellar sources due to the prevalence of
H₂O ice in the cold outer regions (18). Specifically,
the ice sample presented in this paper is composed by
a H₂O:CH₄:NH₃ (2:1:1) mixture, coated with a layer
of mixed CO and CH₃OH (3:1), and exposed to soft
X-rays. We note that a higher relative abundance of
H₂O in the ice, similar to the median values in as-
tronomical observations (3), leads to a more efficient
formation of ultraviolet photoproducts (16, 20), but
this composition is expected to be less representative
of the ice found near the protostar, where X-rays per-
meate the ice.

Because ultraviolet photons have a penetration of a few
hundred monolayers in the ice, where a monolayer corresponds
to the thickness of one molecule and a column density of about
10¹⁵ molecules cm⁻², the present mantle configuration is very
suitable to the deeply penetrating soft X-rays, allowing to
study in detail the formation, and eventual photo-desorption
of radiolysis products. In the ice mixtures studied to date

Significance Statement

Of the over 200 molecules observed in the tenuous gas filling the space between stars, many are organic. Such species mostly form in simple molecular ices coating dust grains in dark interstellar regions. Understanding the production of organics in the early stages of star formation, is critical to tracing the evolution from simple molecules to potentially life-bearing chemistry. Laboratory experiments have shown that a complex chemistry can originate in ices. We experimentally studied the formation and ejection into the gas-phase of organics in ice analogues irradiated by X-rays, obtaining results in close agreement with ALMA observations of protoplanetary disks. X-rays from young solar-type stars are thousands of times higher than today Sun with chemical implications so far relatively unexplored.

Please provide details of author contributions here.

The authors declare no competing interests.

¹To whom correspondence should be addressed. E-mail: angela.ciaravella@inaf.it

(12, 13, 21), the identified X-ray products are common to the ultraviolet experiments. The main focus of this work is, therefore, to follow the destruction of the original ice components, the formation of products in the realistic ice analogs, and their release into the gas phase. **Particular attention is paid to the desorption of molecules during the irradiation, since this allows comparison with the recent observations of protoplanetary disks using the Acatama Large Millimeter Array (ALMA). Young solar-type stars are powerful sources of X-rays, thousands of times brighter than our middle-aged Sun ($\sim 10^{27}$ erg s^{-1}), with chemical implications on the surrounding disks so far relatively unexplored. X-ray emission in such stars fades with age but overcomes the extreme ultraviolet emission up to 1 Gyr (22), and penetrate the disk up to larger distances. X-rays emitted by a typical T Tauri star propagate near the denser region of the disk midplane well beyond 10 AU and the CO snowline, where the ultraviolet radiation is inhibited (23). Thus, X-rays cover a larger temperature gradient and a broader grain size distribution up to few micron-sized dust particles. ALMA allows the detailed observation of various molecules in the gas at different locations within these disks. These maps of observed molecular abundances are confronted with our experimental findings to, first, test the validity of the ice mantle model, and second, elucidate the physical conditions in the disk, such as dust temperature and radiation dose experienced by molecules in the ice, accounting for chemical evolution and the delivery of molecules to the surrounding gas. The detection of more refractory products like COMs and the effect of warm-up of the processed ice is left for a follow-up paper. These COMs are more difficult to identify in the observations, and the more simple species are therefore better proxies of the disk evolution.**

Experiments and Results

A first ice layer containing a mixture of $H_2O:CH_4:NH_3$ (2:1:1) was covered by a second layer composed of a $CO:CH_3OH$ (3:1) mixture. This realistic ice sample was irradiated for 120 min with a soft X-ray spectrum covering the 250 – 1250 eV energy range, and providing 7.6×10^{14} photons s^{-1} . The spectra of the ice during the irradiation are shown in the left panel of Figure 1. In the right panel the column densities of CO and CH_3OH are shown, normalized to their initial values after each irradiation step.

Of the initial 156 ML (1 ML = 10^{15} molecules cm^{-2}) of CH_3OH only 11 ML are left after 20 min irradiation (fourth step). Thus, about 93% of the initial methanol in the ice is destroyed. In the same irradiation time CO is reduced by 45% from 569 to 312 ML. The contribution to CO and CH_3OH from the bottom layer has been estimated in an accompanying experiment performed exploiting a single layer $H_2O:CH_4:NH_3$ mixtures. **The column densities estimated from our experiment are upper limits as in the two layers experiment the radiation impinging on the bottom layer is reduced by the absorption of the top layer. Thus, the contributions to CO and CH_3OH are at most 4 and 10% after 20 min of irradiation, and 12 and 2% at the end of the irradiation, respectively. The CO column density also includes contribution from CH_3OH dissociation during the irradiation. In a protoplanetary disk around a T Tauri star in the region in which the temperature is ≤ 30 K (i.e. beyond 50 AU) the predicted X-ray flux is $\leq 10^{-3}$**

erg $cm^{-2} s^{-1}$ (23). Thus, the same amount of energy experienced by our sample in 20 min would require a time $\geq 4 \times 10^5$ yr, compatible with the lifetime of circumstellar disks (24).

The steep destruction of the methanol in the top layer could be ascribed to the formation of new species and/or photo-desorption. In Figure 2 are the mass-to-charge (m/z) signals of parent molecules ($m/z = 28$ and 31 for CO and CH_3OH) and of the main products of the top layer HCO, H_2CO , CO_2 ($m/z = 29, 30,$ and 44) desorbing during the irradiation. The most intense fragment of methanol $m/z = 31$ was selected considering that $m/z = 32$ can be dominated by O_2 molecules. The largest photo-desorption is detected for $m/z = 28$ related to CO. $m/z = 29$ is larger than expected for the carbon monoxide isotopologue (^{13}CO), and it is representative of the unreacted HCO radicals detected in the infrared spectra at 1848 cm^{-1} , or the main fragment of formaldehyde ($m/z = 30$). CO_2 is the main product photo-desorbing from the top layer and $m/z = 44$ is the second most intense photo-desorbing mass. The spectrum of $m/z = 31$ is very noisy, testifying that photo-desorption of methanol is negligible and suggesting that methanol contribution to the synthesis of new species must be mainly responsible for its destruction. **Methanol contribution to $m/z = 29$ is thus negligible.** H_2CO ($m/z = 30$) is one of the major products of the irradiation (20, 25) of a CH_3OH ice; in Figure 2 its photo-desorption is much higher than that of the CH_3OH parent molecule.

The mass spectra in Figure 2 show an abnormal behaviour as compared to the typical X-ray photo-desorption spectra in which the desorption peaks decrease monotonically during the irradiation (12, 13). In all masses a significant increase of the desorption appears at the fourth irradiation step suggesting a possible contribution from species produced in the bottom layer. This hypothesis has been investigated by running a second experiment in which isotopologues of methane ($^{13}CH_4$) and ammonia ($^{15}NH_3$) have been used in the bottom layer mixture.

In the top panel of Figure 3 the spectra of $m/z = 31$ are reported for the experiments with and without isotopologues in the bottom layer. The two profiles are similar but from the fourth irradiation step the bottom layer products start dominating the photo-desorption. The species contributing to $m/z = 31$ in the experiment with isotopologues is formaldehyde ($H_2^{13}CO$) produced in the bottom layer. The photo-desorption of formaldehyde from the bottom layer is confirmed by the comparison of $m/z = 30$ (H_2CO) and 31 ($H_2^{13}CO$) in the experiments without and with isotopologues, shown in the bottom panel of Figure 3. While desorption of formaldehyde from the top layer dominates the first three irradiation steps, the component coming from the bottom layers takes over after the fourth irradiation step. Desorption of species from the bottom layer implies that bulk diffusion occurred in the ice during irradiation. Given the small size of the X-ray spot (0.08 cm^2) as compared to the ice surface (~ 5 cm^2), we exclude contribution of the bottom layer from the ice edges.

Discussion and Conclusions

The penetration depth of X-rays allows to process dust particles of a few micron. A direct outcome of this effect in

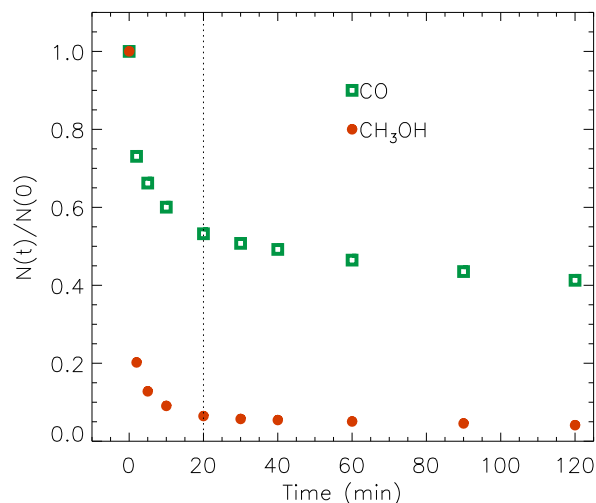
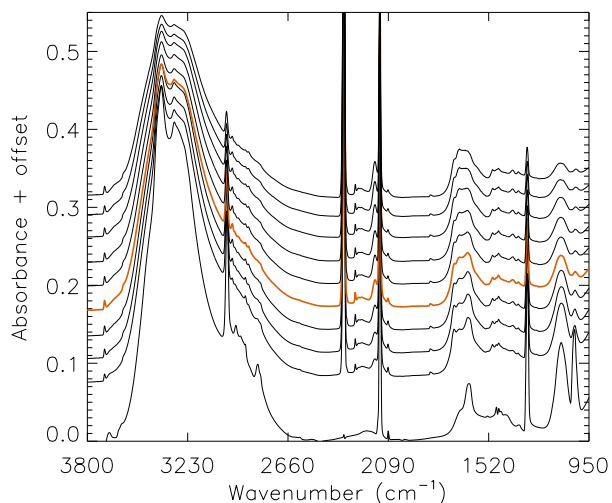


Fig. 1. Left panel: infrared spectra of the bilayer ice before irradiation (bottom curve) and after each irradiation step. The orange spectrum is obtained after the fourth irradiation step. The spectra have been shifted for clarity. Right panel: column densities of CO and CH₃OH normalized to their initial values as functions of the irradiation time. The vertical dotted line marks the fourth irradiation step.

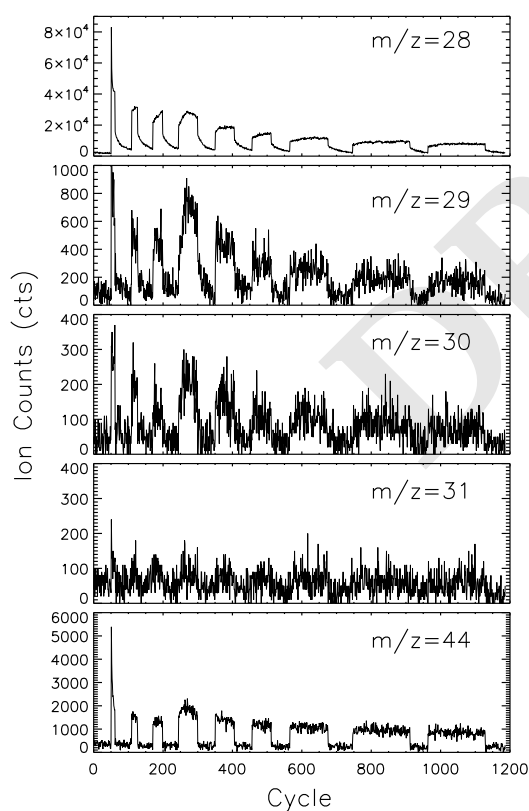


Fig. 2. Ion current vs. cycle detected by the mass spectrometer during the nine irradiation steps for the parent molecules $m/z = 28$ (CO) and 31 (CH₃OH), and for the main products of the top layer HCO, H₂CO, CO₂ ($m/z = 29, 30,$ and 44). The increase of the desorption at the fourth irradiation step marks the contribution of the bottom layer.

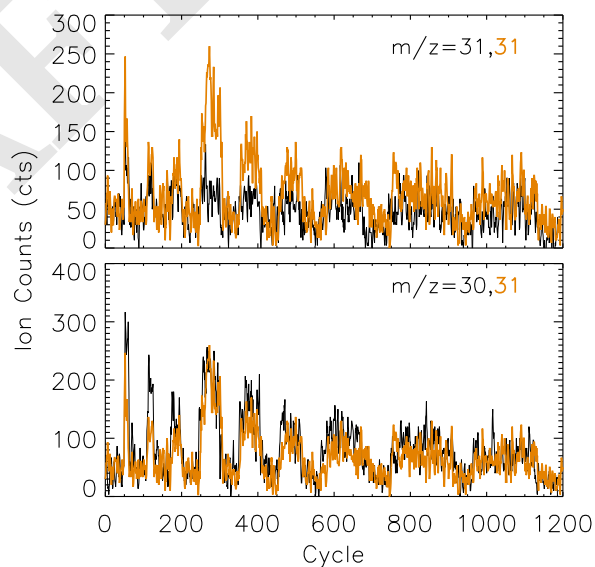


Fig. 3. Top: mass spectra of $m/z = 31$ with (orange) and without (black) isotopologues. From the fourth irradiation step the desorption of H₂¹³CO is detected. Bottom: comparison of $m/z = 30$ (H₂CO) and 31 (H₂¹³CO) in the experiments without and with isotopologues.

X-ray experiments is the high production and release of H₂ from the dissociation of ice molecules such as H₂O and CH₃OH (12), which should contribute to the H₂ abundances observed in disks around young stars (26). Several other species were identified in circumstellar disks, these include H₂O, CO, CO₂, HCO⁺, H₂CO, HCOOH, C₂H, C₂H₂, C₃H₂, CN, HCN, CH₃CN, HC₃N, N₂H⁺, SO, SO₂, and CS (27–34). It was proposed that CO is locked in ice mantles below 30 K, where it can form CH₃OH, CO₂ and/or hydrocarbons (35). H₂CO in the gas was related to a formation by hydrogenation

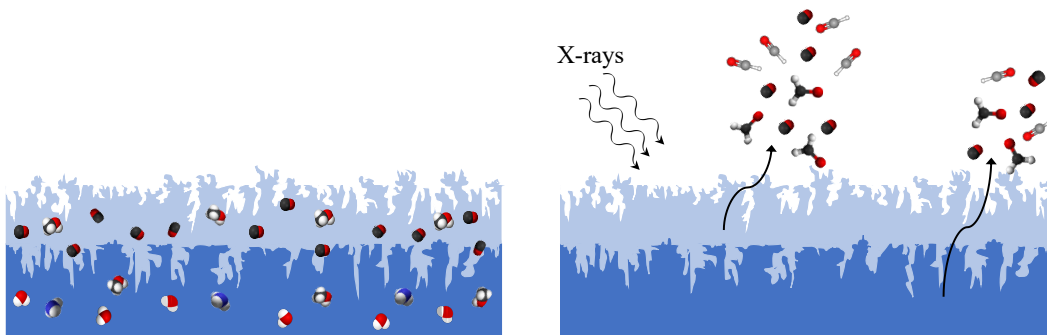


Fig. 4. Sketch of the bilayer ice experiment. Left: the bottom $\text{H}_2\text{O}:\text{CH}_4:\text{NH}_3$ (2:1:1) mixture covered by a layer of $\text{CO}:\text{CH}_3\text{OH}$ (3:1). Right panel: X-ray irradiation of the ice induces a very fast destruction of CH_3OH leading to the formation of new species rather than its photo-desorption. During the irradiation a negligible desorption of CH_3OH has been detected, while CO and products such as HCO, H_2CO and CO_2 show the most intense desorption signals. Desorption from the bottom layer species was also detected.

190 of CO in the dust to match the disk observations (36). The
 191 detection of methanol in the cold gas of protoplanetary disks is
 192 considered a product of ice chemistry (37). The identification
 193 of CH_3OH and other complex species in FUors protostars (38)
 194 strongly support the role of ices in the synthesis of COMs in
 195 space. The protoplanetary disk of young Herbig Ae star HD
 196 163296 presents a much lower methanol-to-formaldehyde ratio
 197 compared to the Class II disk of T Tauri star TW Hya. Among
 198 other possibilities, this could be attributed to differences in the
 199 stellar irradiation, uncertainties in the grain surface formation
 200 and desorption efficiencies of CH_3OH and H_2CO (39).

201 In this work we have experimentally simulated for the
 202 first time a realistically stratified ice mantle surrounding
 203 dust grains by making a double layer ice in which a mixture
 204 of $\text{H}_2\text{O}:\text{CH}_4:\text{NH}_3$ was covered by a second mixture of
 205 $\text{CO}:\text{CH}_3\text{OH}$ (see Figure 4). Such an ice was irradiated with
 206 soft X-rays of energy spectrum in the range 250 – 1250 eV. In
 207 the experiments CH_3OH is rapidly converted to new species,
 208 being H_2CO , HCO and CO the most abundant ones. Photo-
 209 desorption of CH_3OH was negligible while a fraction of the new
 210 species was found to desorb during the X-ray irradiation at 11
 211 K. A similar experiment using the isotopologues $^{13}\text{CH}_4$ and
 212 $^{15}\text{NH}_3$ demonstrated that photo-desorption is not a surface
 213 phenomenon only. Indeed, during the irradiation ion current
 214 of mass-to-charge ratio corresponding to CO, HCO, H_2CO
 215 and CO_2 all have contribution from bottom layer species that
 216 found their way to the surface of the ice. The obtained results
 217 can explain the non-detection of methanol in the gas toward
 218 disk regions exposed to radiation and, meanwhile, the presence
 219 of CO, HCO, and H_2CO . Other hydrogenated species like
 220 H_2O , CH_4 and NH_3 present in the first accreted ice layer are
 221 efficiently processed as well by X-rays, but their products are
 222 to a much lesser extent ejected to the gas. As far as we know
 223 this is the first experiment in which desorption of species from
 224 the bottom layer is detected, implying that bulk diffusion
 225 occurred during X-ray irradiation. Bulk diffusion is highly
 226 relevant for the formation of complex species in ice mantles,
 227 and has received attention both theoretically (40, 41) and exper-
 228 imentally (42, 43). A detailed analysis of the bulk diffusion
 229 in the present experiments is beyond the scope of this work,
 230 and we defer a detailed analysis to a dedicated paper.

231 In summary, the absence or low abundance of complex
 232 species from the cold gas in protoplanetary disks, and the

233 presence of abundant CO, HCO, H_2CO and negligible
 234 CH_3OH is compatible with the X-ray processing of real-
 235 istic ice mantles in the disks around young stars. Moreover,
 236 the experimental simulations are also compatible with low
 237 abundances of other COMs in the cold parts of the disk, since
 238 they are formed in the ice bulk but are not ejected into the
 239 gas phase.

240 Methods

241 The experiments were performed with the Interstellar
 242 Energetic-Process System (44) ultra-high vacuum chamber
 243 at a base pressure of $< 5 \times 10^{-10}$ mbar. The chamber is
 244 equipped with a Quadrupole Mass Spectrometer (QMS) and a
 245 mid infrared spectrometer. This set-up was connected to the
 246 BL08B soft X-ray beamline at National Synchrotron Radia-
 247 tion Research Center (NSRRC, Taiwan), providing a flux of
 248 7.6×10^{14} photons s^{-1} covering the energy range 250 – 1250 eV.
 249 The ice was made of a $\text{H}_2\text{O}:\text{CH}_4:\text{NH}_3$ (2:1:1) mixture covered
 250 by a top layer of $\text{CO}:\text{CH}_3\text{OH}$ (3:1) mixture deposited onto a
 251 CaF_2 substrate at 12 K, which allowed infrared spectroscopy
 252 of the ice samples in transmittance. H_2O from Merck, LC MS
 253 grade, CH_4 from Matheson TRI- GAS 99.999%, NH_3 from
 254 Specialty gases of America, 99.99%, CO from CINGFONG
 255 GAS INDUSTRIAL, purity 99.99%, and CH_3OH from Merck,
 256 99.9%. A similar experiment with a bottom layer made of
 257 $\text{H}_2\text{O}:\text{CH}_4:\text{NH}_3$ was also performed. $^{13}\text{CH}_4$ from Specialty
 258 gases of America, ^{13}C atom 99%, $^{15}\text{NH}_3$ from Cambridge Iso-
 259 tope Laboratories, INC., 98% atom ^{15}N . The QMS was used
 260 for monitoring the gas-phase components in the chamber dur-
 261 ing deposition and the desorbing molecules during irradiation.
 262 The ice samples were irradiated in nine steps (2, 3, 5, 10, 10, 10,
 263 20, 30, 30 min) for a total of 120 minutes. At the end of each
 264 step infrared spectra were collected. The ice column density
 265 was computed as the sum of bottom $N_{\text{H}_2\text{O}} + N_{\text{CH}_4} + N_{\text{NH}_3}$,
 266 and top $N_{\text{CO}} + N_{\text{CH}_3\text{OH}}$ layers from integration of the bands
 267 using the expression

$$268 \quad N = \frac{1}{A} \int_{\text{band}} \tau_\nu d\nu \quad [1] \quad 269$$

270 where N is the column density in cm^{-2} , τ_ν the optical depth of
 271 the band, $d\nu$ the wavenumber differential in cm^{-1} , and A the
 band strength in cm molecule^{-1} . The integrated absorbance

is $0.43 \times \tau$, where τ is the integrated optical depth of the band. In the ice sample without isotopologues the bottom ($N_{\text{H}_2\text{O}} + N_{\text{CH}_4} + N_{\text{NH}_3}$) and the top ($N_{\text{CO}} + N_{\text{CH}_3\text{OH}}$) layers were 1646 and 724 ML, respectively. In the ice sample with isotopologues the bottom ($N_{\text{H}_2\text{O}} + N_{13\text{CH}_4} + N_{15\text{NH}_3}$) and the top ($N_{\text{CO}} + N_{\text{CH}_3\text{OH}}$) layers were 1725 and 775 ML, respectively. The column density of H_2O was computed from the band at 3280 cm^{-1} and a band strength of $2.0 \times 10^{-16} \text{ cm molecule}^{-1}$ (45). The band at 1304 cm^{-1} and a band strength $8.0 \times 10^{-18} \text{ cm molecule}^{-1}$ were used for N_{CH_4} (46). Ammonia N_{NH_3} was computed using the feature at 1112 cm^{-1} and a band strength $1.7 \times 10^{-17} \text{ cm molecule}^{-1}$ (47). The column density of carbon monoxide was obtained by integration of the band at 2138 cm^{-1} and a band strength of $1.1 \times 10^{-17} \text{ cm molecule}^{-1}$ (48). Methanol $N_{\text{CH}_3\text{OH}}$ was computed using the feature at 1026 cm^{-1} and a band strength $1.8 \times 10^{-17} \text{ cm molecule}^{-1}$ (49).

ACKNOWLEDGMENTS. We acknowledge the NSRRC general staff for running the synchrotron radiation facility. We also thank Dr. T.-W. Pi, the spokesperson of BL08B in NSRRC. The Spanish Ministry of Science, Innovation and Universities supported this research under grant number AYA2017-85322-R (AEI/FEDER, UE), and MDM-2017-0737 Unidad de Excelencia "María de Maeztu"-Centro de Astrobiología (INTA-CSIC). We also acknowledge support from the PRIN-INAF 2016 The Cradle of Life - GENESIS-SKA, and the MOST grant MOST 107-2112-M-008-016-MY3 from Taiwan.

1. E Dartois, The Ice Survey Opportunity of ISO. *Space Sci. Rev.* **119**, 293–310 (2005).
2. KI Öberg, et al., The Spitzer Ice Legacy: Ice Evolution from Cores to Protostars. *The Astrophys. J.* **740**, 109 (2011).
3. ACA Boogert, PA Gerakines, DCB Whittet, Observations of the icy universe. *Annu. Rev. Astron. Astrophys.* **53**, 541–581 (2015).
4. EM Penteado, et al., Spectroscopic constraints on CH_3OH formation: CO mixed with CH_3OH ices towards young stellar objects. *Mon. Notices Royal Astron. Soc.* **454**, 531–540 (2015).
5. N Watanabe, A Kouchi, Efficient Formation of Formaldehyde and Methanol by the Addition of Hydrogen Atoms to CO in H_2O -CO Ice at 10 K. *The Astrophys. J. Lett.* **571**, L173–L176 (2002).
6. KI Öberg, Photochemistry and astrochemistry: photochemical pathways to interstellar complex organic molecules. *Chem. Rev.* **116**, 9631–9663 (2016).
7. GM Muñoz Caro, et al., Amino acids from ultraviolet irradiation of interstellar ice analogues. *Nature* **416**, 403–406 (2002).
8. MP Bernstein, JP Dworkin, SA Sandford, GW Cooper, LJ Allamandola, Racemic amino acids from the ultraviolet photolysis of interstellar ice analogues. *Nature* **416**, 401–403 (2002).
9. C Meinert, et al., Ribose and related sugars from ultraviolet irradiation of interstellar ice analogs. *Science* **352**, 208–212 (2016).
10. Y Oba, Y Takano, H Naraoka, N Watanabe, A Kouchi, Nucleobase synthesis in interstellar ices. *Nat. Commun.* **10**, 4413 (2019).
11. Z Kaňuchová, et al., Synthesis of formamide and isocyanic acid after ion irradiation of frozen gas mixtures. *Astron. Astrophys.* **585**, A155 (2016).
12. A Jiménez-Escobar, et al., X-Ray Photo-desorption of $\text{H}_2\text{O}:\text{CO}:\text{NH}_3$ Circumstellar Ice Analogs: Gas-phase Enrichment. *The Astrophys. J.* **868**, 73 (2018).
13. A Ciaravella, et al., Synthesis of Complex Organic Molecules in Soft X-Ray Irradiated Ices. *The Astrophys. J.* **879**, 21 (2019).
14. AGGM Tielens, AT Tokunaga, TR Geballe, F Baas, Interstellar Solid CO: Polar and Nonpolar Interstellar Ices. *The Astrophys. J.* **381**, 181 (1991).
15. KM Pontoppidan, et al., The c2d Spitzer Spectroscopic Survey of Ices around Low-Mass Young Stellar Objects. II. CO_2 . *The Astrophys. J.* **678**, 1005–1031 (2008).
16. GM Muñoz Caro, WA Schutte, UV-photoprocessing of interstellar ice analogs: New infrared spectroscopic results. *Astron. Astrophys.* **412**, 121–132 (2003).
17. P de Marcellus, et al., Photo and thermochemical evolution of astrophysical ice analogues as a source for soluble and insoluble organic materials in Solar system minor bodies. *Mon. Notices Royal Astron. Soc.* **464**, 114–120 (2017).
18. PA Gerakines, MH Moore, RL Hudson, Energetic Processing of $\text{H}_2\text{O}:\text{CH}_3\text{OH}:\text{CO}_2$ Interstellar Ice Analogs: UV Photolysis vs. Ion Bombardment in *American Astronomical Society Meeting Abstracts*, American Astronomical Society Meeting Abstracts. Vol. 195, p. 128.06 (1999).
19. E Dartois, et al., Methanol: The second most abundant ice species towards the high-mass protostars RAFGL7009S and W 33A. *Astron. Astrophys.* **342**, L32–L35 (1999).
20. KI Öberg, RT Garrod, EF van Dishoeck, H Linnartz, Formation rates of complex organics in UV irradiated CH_3OH -rich ices. I. Experiments. *Astron. Astrophys.* **504**, 891–913 (2009).
21. GM Muñoz Caro, et al., X-Ray versus Ultraviolet Irradiation of Astrophysical Ice Analogs Leading to Formation of Complex Organic Molecules. *ACS Earth Space Chem.* **3**, 2138 (2019).
22. I Ribas, EF Guinan, M Güdel, M Audard, Evolution of the solar activity over time and effects on planetary atmospheres. I. high-energy irradiances (1–1700 Å). *Astrophys. J.* **622**, 680–694 (2005).

23. C Walsh, H Nomura, TJ Millar, Y Aikawa, Chemical Processes in Protoplanetary Disks. II. On the Importance of Photochemistry and X-Ray Ionization. *The Astrophys. J.* **747**, 114 (2012).
24. AJW Richert, et al., Circumstellar disc lifetimes in numerous galactic young stellar clusters. *Mon. Notices Royal Astron. Soc.* **477**, 5191–5206 (2018).
25. YJ Chen, et al., Soft X-Ray Irradiation of Methanol Ice: Formation of Products as a Function of Photon Energy. *The Astrophys. J.* **778**, 162 (2013).
26. TL Beck, JS Bary, A Search for Spatially Resolved Infrared Rovibrational Molecular Hydrogen Emission from the Disks of Young Stars. *The Astrophys. J.* **884**, 159 (2019).
27. F Lahuis, et al., Hot Organic Molecules toward a Young Low-Mass Star: A Look at Inner Disk Chemistry. *The Astrophys. J. Lett.* **636**, L145–L148 (2006).
28. C Qi, KI Öberg, DJ Wilner, KA Rosenfeld, First Detection of $\text{c-C}_3\text{H}_2$ in a Circumstellar Disk. *The Astrophys. J. Lett.* **765**, L14 (2013).
29. KI Öberg, et al., The comet-like composition of a protoplanetary disk as revealed by complex cyanides. *Nature* **520**, 198–201 (2015).
30. L Podio, et al., The jet and the disk of the HH 212 low-mass protostar imaged by ALMA: SO and SO_2 emission. *Astron. Astrophys.* **581**, A85 (2015).
31. MT Carney, et al., Increased H_2CO production in the outer disk around HD 163296. *Astron. Astrophys.* **605**, A21 (2017).
32. C Favre, et al., First Detection of the Simplest Organic Acid in a Protoplanetary Disk. *The Astrophys. J. Lett.* **862**, L2 (2018).
33. AS Booth, et al., Sulphur monoxide exposes a potential molecular disk wind from the planet-hosting disk around HD 100546. *Astron. Astrophys.* **611**, A16 (2018).
34. AS Booth, C Walsh, JD Ilee, First detections of H^{13}CO^+ and HC^{15}N in the disk around HD 97048. Evidence for a cold gas reservoir in the outer disk. *Astron. Astrophys.* **629**, A75 (2019).
35. AD Bosman, C Walsh, EF van Dishoeck, CO destruction in protoplanetary disk midplanes: Inside versus outside the CO snow surface. *Astron. Astrophys.* **618**, A182 (2018).
36. L Podio, et al., Organic molecules in the protoplanetary disk of DG Tauri revealed by ALMA. *Astron. Astrophys.* **623**, L6 (2019).
37. C Walsh, et al., First Detection of Gas-phase Methanol in a Protoplanetary Disk. *Astrophys. J. Lett.* **823**, L10 (2016).
38. JE Lee, et al., The ice composition in the disk around V883 Ori revealed by its stellar outburst. *Nat. Astron.* **3**, 314–319 (2019).
39. MT Carney, et al., Upper limits on CH_3OH in the HD 163296 protoplanetary disk. Evidence for a low gas-phase CH_3OH -to- H_2CO ratio. *Astron. Astrophys.* **623**, A124 (2019).
40. HM Cuppen, et al., Grain Surface Models and Data for Astrochemistry. *Space Sci. Rev.* **212**, 1–58 (2017).
41. P Ghesquière, et al., Diffusion of molecules in the bulk of a low density amorphous ice from molecular dynamics simulations. *Phys. Chem. Chem. Phys. (Incorporating Faraday Transactions)* **17**, 11455–11468 (2015).
42. F Mispelaer, et al., Diffusion measurements of CO, HNC, H_2CO , and NH_3 in amorphous water ice. *Astron. Astrophys.* **555**, A13 (2013).
43. P Ghesquière, A Ivlev, JA Noble, P Theulé, Reactivity in interstellar ice analogs: role of the structural evolution. *Astron. Astrophys.* **614**, A107 (2018).
44. CH Huang, et al., Effects of 150–1000 eV Electron Impacts on Pure Carbon Monoxide Ices Using the Interstellar Energetic-Process System (IEPS). *The Astrophys. J.* **889**, 57 (2020).
45. PA Gerakines, WA Schutte, JM Greenberg, EF van Dishoeck, The infrared band strengths of H_2O , CO and CO_2 in laboratory simulations of astrophysical ice mixtures. *Astron. Astrophys.* **296**, 810 (1995).
46. M Bouilloud, et al., Bibliographic review and new measurements of the infrared band strengths of pure molecules at 25 K: H_2O , CO_2 , CO, CH_4 , NH_3 , CH_3OH , HCOOH and H_2CO . *Mon. Notices Royal Astron. Soc.* **451**, 2145–2160 (2015).
47. SA Sandford, LJ Allamandola, Condensation and Vaporization Studies of CH₃OH and NH₃ Ices: Major Implications for Astrochemistry. *The Astrophys. J.* **417**, 815 (1993).
48. GJ Jiang, WB Person, KG Brown, Absolute infrared intensities and band shapes in pure solid CO and CO in some solid matrices. *J. Chem. Phys.* **62**, 1201–1211 (1975).
49. PA Gerakines, WA Schutte, P Ehrenfreund, Ultraviolet processing of interstellar ice analogs. I. Pure ices. *Astron. Astrophys.* **312**, 289–305 (1996).